Front Wheel Shimmy Control Method of Electric Wheel Vehicles Based on Homogeneous Domination

Chao Wang, Qinghua Meng*

School of Mechanical Engineering, Hangzhou Dianzi University, Hangzhou, 310018, China (e-mail: 812286109@qq.com, mengqinghua@hdu.edu.cn).

Abstract: The hub motor has been applied to new energy vehicles due to its excellent performance, but the hub motor increases the unsprung mass and changes the tire dynamic characteristics of the vehicle. This change makes the front wheel shimmy phenomenon more prone to occur, which further influences the vehicle's stability, comfort, fuel efficiency, and safety. Therefore, it is highly necessary to apply modern control theory to the shimmy control. This paper addresses the issue of front wheel shimmy occurring when electric wheeled vehicles are traveling on roads, in addition to the problem of unknown measurement errors in sensors. We established a one-degree-of-freedom model for front wheel shimmy, derived the state equations of the model, and designed a state observer and output feedback controller based on homogeneous domination control theory. Using the Lyapunov function method, it is proven that the designed controller can globally asymptotically stabilize the system. Finally, the designed homogeneous domination controller for the front wheel shimmy system was simulated using MATLAB and then compared with sliding mode control. The results demonstrate that the proposed method in this paper can effectively eliminate the front wheel shimmy phenomenon and has good robustness.

Keywords: Front wheel shimmy, homogeneous domination control, electric wheel vehicle, vehicle dynamics, vehicle stability.

1. INTRODUCTION

Front wheel shimmy refers to the phenomenon where the front wheels continuously oscillate around the kingpin while the vehicle is traveling on the road. This vibration is transmitted through the steering system to the steering wheel, causing the entire vehicle to experience shimmying (Wang et al., 2024; Meng et al., 2024). In recent years, the global automotive industry has been developing towards new energy vehicles, particularly electric wheeled vehicles independently driven by hub motors (Zhuang, 2020). While the application of hub motors has eliminated many transmission components, improving transmission efficiency, it also changes the tire dynamics characteristics, which makes the front wheel shimmy phenomenon more likely to occur (Wu et al., 2023). It significantly impacts the vehicle's driving stability, safety, and motor life. Therefore, it is urgent to study the mechanisms, influencing factors, and the active control methods of vehicle shimmy.

Many scholars have conducted extensive research on the mechanism of shimmy, yielding a series of achievements. (Becker et al., 1931) invented the tire beam formula, and carried out experiments on this basis, found that the lateral force is an important factor affecting the shimmy. (Pacejka, H.B., 1966) analyzed the relationship between tire slip angle, lateral forces applied to the wheels, and the self-aligning torque of the wheels. On this basis, he derived the widely recognized tire magic formula, which has been extensively used in shimmy research. Subsequently, (Pacejka, H.B., 1973) further improved the magic formula tire model using a frequency response characteristic calculation method, enhancing accuracy and closely aligning with experimental results. After summarizing and revising the previous magic formula tire model, (Bakker et al., 1987) introduced a semi-empirical tire magic formula that effectively reflects the dynamic characteristics of tires during vehicle motion. It has been widely applied and referenced in research. (Demic, M., 1996) analyzed the impact of design parameters on the shimmy of steering wheels in heavy-duty vehicles. (Guo et al., 1986) proposed a semi-empirical model for tire lateral characteristics through extensive research and experiments. (Guo, K.H., 1995) further investigated the impact of dynamic tire lateral characteristics on vehicle shimmy, revealing that larger wheel radius, greater kingpin inclination angle, and higher cornering stiffness, coupled with lower tire lateral stiffness, tend to increase the tendency of shimmy. (Wang et al., 2012) established a nonlinear three-degree-of-freedom shimmy system and conducted simulations, analyzing the impact of tire vertical stiffness, tire lateral stiffness, damping of wheel rotation around the kingpin, and tire trail on shimmy. (Wei et al., 2022) considering stochastic clearances, analyzed the influence of clearance nodes on the dynamic characteristics of a six-degree-of-freedom vehicle shimmy system based on a dynamic model. (Lu et al., 2023) developed a vehicle dynamics model considering the coupling mechanism

* Corresponding author, Qinghua Meng.

between front wheel shimmy and lateral vehicle motion, studying the interaction effects between steering shimmy and overall vehicle motion instability. The research focused on the impact of tire force saturation caused by different degrees of lateral and longitudinal coupling on braking force distribution strategy.

It is evident from the aforementioned studies that the methods for solving vehicle shimmy problems are fundamentally based on dynamics. Researchers investigate the relationships between various parameters and shimmy, aiming to reduce or eliminate shimmy by altering fixed parameter values. The method involves designing a rational mechanical structure during vehicle manufacturing. If factors such as wear, deformation, or displacement occur between components during the subsequent use of the vehicle, affecting certain parameters that influence shimmy, adjusting the vehicle's inherent parameters becomes challenging. As time and technology progress, it is necessary to use modern control theory to design an active control method for suppressing shimmy. Unfortunately, there are currently few such achievements, with the primary focus of research being on shimmy in aircraft landing gear (Wang et al., 2022; Wang et al., 2023; Dong et al., 2023). (Xiao, 2022) proposed a steering wheel shimmy suppression controller based on rack force estimation, effectively reducing the impact of shimmy on steering feel and enhancing driving comfort. (Meng et al., 2019) established a new two-degree-of-freedom shimmy model for the independent suspension of electric vehicles under uncertain disturbances. He proposed an active control method using sampled data output feedback control to address shimmy problems. Furthermore, (Meng et al., 2020) constructed a four-degree-of-freedom shimmy model for electric wheeled vehicles with independent suspension. He proposed an active shimmy control method based on disturbance estimation observer with finite time. Based on spatial rod system configuration parameters, (Zhou, 2022) developed an optimized control model for vehicle shimmy. The study utilized multi-objective particle swarm optimization analysis, achieving research on vehicle shimmy control optimization based on spatial rod system configuration parameters in a multi-rigid-body dynamics environment.

In recent years, many scholars have proposed numerous advanced control methods with excellent control performance, potentially applicable to shimmy control. (Zhang et al., 2023) proposed an adaptive fixed-time backstepping control method utilizing a command-filtering technique and an adaptive disturbance observer, which can effectively estimate total interference with minimal error. (Ata and Coban, 2022) proposed a decoupling algorithm with combination of sliding mode control and adaptive backstepping control. (Kchaou et al., 2022) proposed a fuzzy output feedback control scheme to address the reliable sampled-data control problem of nonlinear systems. (Qian and Li, 2006) proposed a homogeneous control method for globally output feedback stabilization of a class of nonlinear systems. This approach exhibits robustness, is suitable for systems with significant uncertainties and strong nonlinearity, and effectively enhances system stability, supported by empirical evidence. (Xie and Liu, 2012) applied homogeneous control methods to solve the state feedback stabilization problem for high-order nonlinear systems with time-varying delays and randomness. (Chen and Xu, 2018) proposed a method based on homogeneous control with added power integrator technology. (Zhao and Su, 2020) further constructed state-dependent homogeneous control stabilizers for p-norm systems with interval power products. (Meng et al., 2021) applied the homogeneous domination control method to the vehicle active suspension system and found its control performance surpasses sliding mode control. (Meng et al., 2023) also employed the homogeneous domination control method in lane-keeping technology, revealing that the controller has strong robustness, fast response speed, and low energy output, making it more suitable for lane-keeping systems and improving their performance.

2. RELATED WORK

Given the advantages of homogeneous control, this paper proposes a homogeneous domination control method for the front-wheel shimmy control of electric wheeled vehicles. The third section details the construction of the dynamic model for front-wheel shimmy in electric wheel vehicles. The fourth section proposes the designed homogeneous domination controller and observer, employing the Lyapunov method to prove the asymptotic stability of the front-wheel shimmy control system. The fifth section applies the homogeneous domination controller and observer to the front-wheel shimmy system and conducts numerical simulations, comparing the results with the sliding mode control method. The sixth section offers concluding remarks on the study.

3. FRONT WHEEL SHIMMY MODEL FOR ELECTRIC WHEEL VEHICLES

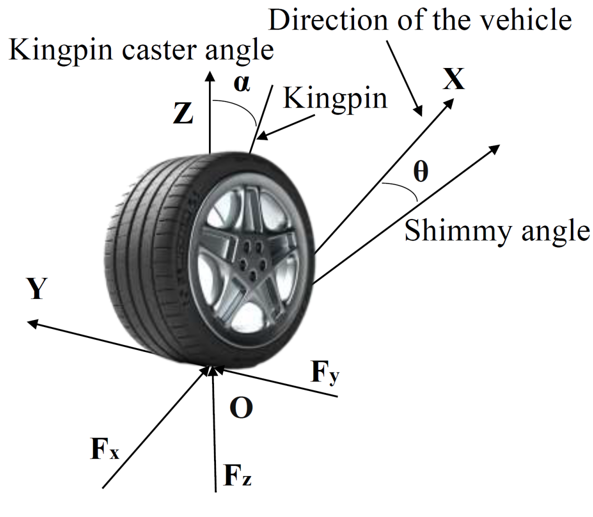

Fig. 1. One-degree-of-freedom front wheel shimmy model

As discussed in the previous section of the literature, it is evident that shimmy typically arises from the interplay of multiple factors. To elucidate the underlying mechanisms, many researchers have developed various shimmy models that are increasingly practical and feature higher degrees of freedom. However, as the degree-of-freedom (DOF) increases, the complexity of the models escalates, concurrently heightening control challenges. Therefore, this

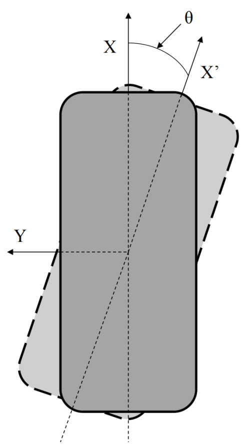

Fig. 2. Top view of tire

paper chooses to establish a one-degree-of-freedom shimmy model for the left front wheel of an electric wheel vehicle, making it easier to simultaneously address unknown sensor measurement errors and nonlinear terms. The model is illustrated in Fig. 1. To better understand what is the shimmy angle, Fig. 2 is a top view of the tire. X-axis represents the direction of the tire when the vehicle is traveling normally. When the vehicle experiences shimmy, as shown in the Fig. 2, the tire rotates clockwise by a certain angle, and at this point, the direction of the tire is X'-axis. The shimmy angle is the angle between X and X'. The derivation of the model will be carried out by Lagrange's theorem as

$$\frac{\mathrm{d}}{\mathrm{d}t}(\frac{\partial T}{\partial \dot{q}}) - \frac{\partial T}{\partial q} + \frac{\partial U}{\partial q} + \frac{\partial D}{\partial \dot{q}} = Q. \tag{1}$$

where T is the kinetic energy of the system, U is the potential energy of the system, D is the dissipated energy of the system, q is the generalized coordinates, Q is the generalized force acting on generalized coordinates. Wherein, the expressions of kinetic energy, potential energy, and dissipative energy of the system are

$$\begin{aligned} T &= \frac{1}{2}J\dot{\theta}^2, \\ U &= \frac{1}{2}L^2 k_s \theta^2 + \frac{1}{2}L^2 k_z \theta^2 \sin\alpha(\sin\alpha + f\cos\alpha), \\ D &= \frac{1}{2}c_l\dot{\theta}^2 + \frac{1}{2}L^2 c_s \dot{\theta}^2. \end{aligned} \tag{2}$$

where J is the moment of inertia of the wheel around its kingpin, θ is the shimmy angle, L is the effective length of the knuckle, k_s is the equivalent torsional angular stiffness of the wheel around kingpin, k_z is the vertical stiffness of tire, α is the kingpin caster angle, f is the rolling resistance coefficient, c_l is the equivalent damping coefficient of the wheel around kingpin, and c_s is the damping coefficient of the electric wheel. In the case of tires, the movement around kingpin is mainly caused by lateral forces and other external disturbances. Therefore, the expression for the generalized force Q is

$$Q = -F_y(t_m + R\sin\alpha) + \Delta - u. \tag{3}$$

where F_y is the lateral force of the tire, and t_m is the drag distance of the tire. R is the wheel rolling radius, Δ is the torque generated by the uncertain disturbance on the left front wheel and kingpin, and u is the output of the controller.

To get more accurate lateral force of a tire, using the computing method given in (He, 2004)

$$F_y = a_1\chi(\theta - b\dot{\theta}) + a_2\chi^2(\theta - b\dot{\theta})^2 + a_3\chi^3(\theta - b\dot{\theta})^3. \tag{4}$$

where

$$\begin{aligned} &\chi = [(\rho v/k)^2 + (\rho f/k)\omega^2]/[\omega^2 + (\rho v/k)^2], \\ &b = [(\rho v/k)^2 - \rho^2 f v/k^2]/[(\rho v/k)^2 + \rho f \omega^2/k], \\ &a_1 = k, a_2 = -0.0668k^2/(\mu \cdot G_z), \\ &a_3 = -0.1032k^3/(\mu \cdot G_z)^2. \end{aligned} \tag{5}$$

where ρ is the lateral stiffness of the tire, v is the vehicle velocity, k is the lateral stiffness of the tire, ω is the natural frequency, G_z is the vertical weight of the front wheel, and μ is the road adhesion coefficient.

Substituting equations (2) to (5) into equation (1) obtains the differential equation for the shimmy of the left front wheel around the kingpin

$$\begin{aligned} &J\ddot{\theta} + [d^2k_s + d^2k_z\sin\alpha(\sin\alpha + f\cos\alpha) \\ &+k\chi(t_m + R\sin\alpha)]\theta + [c_l + d^2c_s \\ &-bk\chi(t_m + R\sin\alpha)]\dot{\theta} - \Delta + u \\ &+[a_1\chi(\theta - b\dot{\theta}) + a_2\chi^2(\theta - b\dot{\theta})^2 \\ &+a_3\chi^3(\theta - b\dot{\theta})^3](t_m + R\sin\alpha) = 0. \end{aligned} \tag{6}$$

Let $x_1(t)$=$\theta(t)$ and $x_2(t)$=$\dot{\theta}(t)$, differential equation (6) can be rewritten as state equation (7), in the following form

$$\begin{aligned} \dot{x}_1(t) &= x_2(t) + \varphi_1(t, x, u), \\ \dot{x}_2(t) &= U(t) + \varphi_2(t, x, u) + M, \\ y &= f(t)x_1(t). \end{aligned} \tag{7}$$

where

$$\begin{aligned} &\varphi_1(t, x, u) = 0, \\ &\varphi_2(t, x, u) = -\frac{1}{J}[d^2k_s + d^2k_z\sin\alpha(\sin\alpha + f\cos\alpha) \\ &+ k\chi(t_m + R\sin\alpha)]x_1 - \frac{1}{J}[c_l + d^2c_s \\ &- bk\chi(t_m + R\sin\alpha)]x_2 + \frac{1}{J}[a_1\chi(x_1 - bx_2) \\ &+ a_2\chi^2(x_1 - bx_2)^2 + a_3\chi^3(x_1 - bx_2)^3](t_m + R\sin\alpha), \\ &U(t) = -\frac{u}{J}, \qquad M = \frac{\Delta}{J}. \end{aligned}$$

4. DESIGN OF HOMOGENEOUS DOMINATION OBSERVER AND CONTROLLER

The initial step involves the establishment of several inequalities, definitions, lemmas, and hypotheses to be utilized in the ensuing proof process. These have been substantiated within pertinent literature.

Hypothesis 1. There exits $\tau \geq 0$ and $c \geq 0$

$$|\phi_i| \leq c(|x_1|^{i\tau+1} + \cdots + |x_i|^{r_i}), i = 1, 2, ... \tag{8}$$

Where $r_i = \frac{i\tau+1}{(i-1)\tau+1}$.

Before giving the lemma, it is necessary to introduce the following definitions (Kawski, M., 1990).

For fixed coordinates $(x_1, \cdots, x_n) \in R^n$ and real numbers $r_i > 0, i = 1, \cdots, n$,

Definition 1: The dilation $\Delta_\xi(x)$ is defined as $(\xi^{r_1} x_1, \cdots, \xi^{r_n} x_n)$, where $\xi > 0$. r_i is called as the weights of the coordinates. In order to make the following writing more concise, the dilation weight is written as $\Delta = (r_1, \cdots, r_n)$.

Definition 2: A function $V \in C(R^n, R)$ is referred to as homogeneous of degree τ if there is a real number $\tau \in R$ such that $\forall x \in R^n \backslash \{0\}, \xi > 0$, $V(\Delta_\xi(x)) = \xi^\tau V(x_1, \cdots, x_n)$.

Definition 3: A homogeneous p-norm is defined as $\|x\|_{\Delta,p} = (\sum_{i=1}^n |x_i|^{p/r_i})^{1/p}$, $\forall x \in R^n$, for a constant $p \geq 1$. In this section, when p=2, $\|x\|_{\Delta,2}$ is written as $\|x\|_\Delta$.

Lemma 2. (Qian, C., 2005). Suppose $V(x) : R^n \to R$ is a homogeneous function of the τ degree with respect to the expansion weight Δ, the following holds:

(1) r_i is the homogeneous weight of x_i, and the homogeneous degree of $\frac{\partial V}{\partial x_i}$ is τ-r_i.

(2)There is a constant C such that

$$V(x) \leq C||x||^\tau_\Delta$$

In particular, if $V(x)$ is positively definite, then for $c > 0$, there is

$$c||x||^\tau_\Delta \leq V(x)$$

Lemma 3. (Qian, C., 2005). Given a dilation weight $\Delta = (r_1, \cdots, r_n)$, suppose $V_1(x)$ and $V_2(x)$ are homogeneous functions of degree τ_1 and τ_2. Then $V_1(x)V_2(x)$ is also homogeneous with respect to the same dilation weight Δ. Moreover, the homogeneous degree of $V_1(x)V_2(x)$ is τ_1+τ_2.

Lemma 4. (Qian and Li, 2006). For x∈R, y∈R , $p \geq 1$, there exists

$$|x + y|^p \leq 2^{p-1}|x^p + y^p|, \tag{9}$$

$$(|x| + |y|)^{1/p} \leq |x|^{1/p} + |y|^{1/p}.$$

If $p \geq 1$ is odd number, there exists

$$|x - y|^p \leq 2^{p-1}|x^p - y^p|. \tag{10}$$

Lemma 5. (Qian and Li, 2006). Let $p \geq 1$ be an odd real number and x, y be real-valued functions. Then,

$$|x^p - y^p| \leq p|x - y|(x^{p-1} + y^{p-1}). \tag{11}$$

The proposed method in this paper aims to solve the problem of unknown sensor measurement error and nonlinearity of the front wheel shimmy control system. Accordingly, leveraging the homogeneous domination control theory (Qian, C., 2005), we have developed a controller (12) and an observer (13). Subsequently, it is demonstrated that this approach ensures the global asymptotic stability of the front wheel shimmy system (7) under Hypothesis (1). The controller is designed as

$$\begin{aligned} u(\hat{x}) &= -\beta_2(\hat{x}_2 + \beta_1 \hat{x}_1^{p_1})^{p_2}, \\ p_1 &= r_2/r_1, \\ p_2 &= (r_2 + \tau)/r_2. \end{aligned} \tag{12}$$

where β_i is a positive constant, r_i is the homogeneous weight of x_i, τ is a homogeneous degree.

The observer is designed as

$$\begin{aligned} \hat{x}_1 &= f(x)x_1, \\ \hat{x}_2 &= (\eta_2 + \eta_1 \hat{x}_1)^{p_1}, \\ \dot{\eta}_2 &= -l_1 \hat{x}_2. \end{aligned} \tag{13}$$

where $l_1 > 0$, $n_i > 0$.

Proof. For simplicity, let $\tau = A/B$, where A is an even number and B an odd number. And then there is

$$r_i = (i - 1)\tau + 1, i = 1, 2, ...$$

which are odd numbers.

Firstly, it need to prove that the homogeneous state feedback controller can globally asymptotically stabilize the following system (14) without unknown nonlinear terms.

$$\begin{aligned} \dot{x}_1 &= x_2, \\ \dot{x}_2 &= u. \end{aligned} \tag{14}$$

Defining u=x_3, a virtual controller

$$x_2^* = -\beta_1 x_1^{\frac{r_2}{r_1}}, \beta_1 = 2 + c_1,$$
$$\psi_1 = x_1 - x_1^*, \psi_2 = x_2 - x_2^*.$$

and select $V_1(x_1) = \frac{r_1}{2r_2 - \tau} x_1^{\frac{2r_2 - \tau}{r_1}}$, there exists

$$\dot{V}_1(x_1, x_2) \leq -2x_1^{\frac{2r_2}{r_1}} + x_1^{\frac{2r_2-\tau}{r_1 - 1}}(x_2 - x_2{}^*). \tag{15}$$

Constructing Lyapunov function

$$V_2(x_1, x_2) = V_1 + \frac{r_2}{2r_2 - \tau} \psi_2^{\frac{2r_2 - \tau}{r_2}}. \tag{16}$$

the derivative of $V_2(x_1, x_2)$ is

$$\begin{aligned} \dot{V}_2(x_1, x_2) \leq\ & -2\psi_1^{2r_2/r_1} + \psi_1^{\frac{2r_2-\tau}{r_1} - 1} \psi_2 \\ & + \psi_2^{\frac{2r_2-\tau}{r_2} - 1}(x_3 + \phi_2(x) - \frac{\partial x_1{}^*}{\partial x_1} \dot{x}_1). \end{aligned} \tag{17}$$

According to the definition of the virtual controller, there exists

$$x_3^* = -\beta_2 \psi_2^{\frac{r_3}{r_2}} = -(1+c_2+\tilde{c}_2)\psi_2^{\frac{r_3}{r_2}} = u = -\beta_2 \psi_2^{\frac{r_2+\tau}{r_2}}. \tag{18}$$

Therefore,

$$\dot{V}_2(x_1, x_2) \leq -(\psi_1^{\frac{2r_2}{r_1}} + \psi_2^2) + \psi_2^{\frac{2r_2-\tau}{r_2} - 1}(u - u^*). \tag{19}$$

Select $u^* = -\beta_2 \psi_2^{\frac{r_2+\tau}{r_2}}$, there is

$$\dot{V}_2(x_1, x_2) \leq -\psi_1^{2r_2/r_1} - \psi_2^2 + \frac{\partial V_1(x_1)}{\partial x_1}\phi_1 + \frac{\partial V_2(x_2)}{\partial x_2}\phi_2. \tag{20}$$

According to Hypothesis 1, there is

$$\begin{aligned} \phi_1 &\leq c(|x_1|^{\tau+1}), \\ \phi_2 &\leq c(|x_1|^{\tau+1} + |x_2|^{\frac{2\tau+1}{\tau+1}}). \end{aligned} \tag{21}$$

Furthermore, it can be concluded that

$$\begin{aligned} \dot{V}_2(x_1, x_2) &\leq -\psi_1^{\frac{2r_2}{r_1}} + \psi_2^2 + 2\chi(\psi_1^{\frac{2r_2}{r_1}} + \psi_2^2) \\ &< -(\psi_1^{\frac{2r_2}{r_1}} + \psi_2^2)(1 - 2\chi). \end{aligned} \tag{22}$$

Choosing a reasonable parameter χ can make $\dot{V}_2(x_1, x_2) < 0$, so the state feedback controller can asymptotically stabilize the front wheel shimmy system (7).

In the shimmy control system, x_1 can be obtained from a sensor, but x_2 can not be obtained directly from a sensor, so an observer is needed to estimate x_2. Therefore, it need to prove that the front wheel shimmy system can be asymptotically stabilized with the designed controller and observer.

Similarly, it is necessary to first prove that the controller and observer can stabilize system without nonlinear terms (14), and then prove that they can asymptotically stabilize the front wheel shimmy system (7).

Constructing C^1 function U_2

$$U_2 = \int_{(\eta_2+\eta_1 x_1)^{\frac{r_2}{r_1}}}^{x_2} (s^{\frac{r_1}{r_2}} - (\eta_2 + \eta_1 x_1))ds. \tag{23}$$

There are

$$\begin{aligned}
\frac{\partial U_2}{\partial x_2} &= x_2^{\frac{r_1}{r_2}} - (\eta_2 + \eta_1 x_1),\\
\frac{\partial U_2}{\partial \eta_2} &= -x_2 + (\eta_2 + \eta_1 x_1)^{\frac{r_2}{r_1}},\\
\frac{\partial U_2}{\partial x_1} &= -\eta_1 (x_2 - (\eta_2 + \eta_1 x_1)^{\frac{r_2}{r_1}}).
\end{aligned}$$

The derivative of U_2 is

$$\begin{aligned}
\dot{U}_2 = \ & x_3(x_2^{\frac{r_1}{r_2}} - (\eta_2 + \eta_1 x_1)) - \eta_1 e_2 (x_2 - \hat{x}_2)\\
& -\eta_1 e_2 (\hat{x}_2 - (\eta_2 + \eta_1 x_1)^{\frac{r1}{r2}}).
\end{aligned} \tag{24}$$

where $x_3 = u(\hat{x})$, $e_2 = x_2 - \hat{x}_2$.

Next, it is necessary to deal with the terms in equation (24).

Because $e_2 = x_2 - \hat{x}_2$, there is

$$-\eta_1 e_2 (x_2 - \hat{x}_2) = -\eta_1 e_2^2. \tag{25}$$

Now, the first term on the right-hand side of the equation (24) needs to be addressed.

$$x_3(x_2^{\frac{r_1}{r_2}} - (\eta_2 + \eta_1 x_1)) = C x_3 x_2 (x_2^{\frac{r_1}{r_2}} - (x_2 - e_2)^{\frac{r_1}{r_2}} - \eta_1 e_1). \tag{26}$$

Because $r_{i-1}/r_i < 1$, according to Lemma 4, there is

$$|x_2^{\frac{r_1}{r_2}} - (x_2 - e_2)^{\frac{r_1}{r_2}}| \le 2^{1-\frac{r_1}{r_2}} |e_2|^{\frac{r_1}{r_2}}. \tag{27}$$

Meanwhile

$$\begin{aligned}
|x_2| &\le |\psi_2| + \beta_1 |\psi_1|^{r_2/r_1},\\
|x_3| &\le |\psi_3| + \beta_2 |\psi_2|^{r_3/r_2}.
\end{aligned} \tag{28}$$

Therefore,

$$\begin{aligned}
x_3(x_2^{\frac{r_1}{r_2}} - (\eta_2 + \eta_1 x_1)) \le & \frac{1}{12}\left(\psi_1^{2r_2/r_1} + \psi_2^2 + \psi_3^{2r_2/r_3}\right)\\
& + \gamma_2 e_2^2 + g_2(\eta_1) e_1^{2r_2/r_1}.
\end{aligned} \tag{29}$$

where γ_2 is a constant and $g_2(\cdot)$=0.

According to the homogeneity, one obtains

$$|u(\hat{x})| \le c||\hat{x}||_{\Delta_x}^{r_2+\tau} \le c||x||_{\Delta_x}^{r_2+\tau} + c||e||_{\Delta_x}^{r_2+\tau}. \tag{30}$$

where $||x||_{\Delta_x} = (\sum_{i=1}^{2} |\hat{x}_i|^{\frac{2}{r_i}})^{1/2}$, $\Delta_x = (r_1, r_2)$.

According to the definition of the homogeneous norm, it is known that

$$\begin{aligned}
||x||_{\Delta_x} &= (|\psi_1^{2/r_1} + |\psi_i - \omega_1 \psi_1^{r_2/r_1}|^{2/r_2})^{1/2}\\
&\le c(\sum_{i=1}^{2} |\psi_i|^{2/r_i})^{1/2} = c||\xi||_{\Delta_x}.
\end{aligned} \tag{31}$$

Thus

$$|u(\hat{x})| \le c||\psi||_{\Delta_x}^{r_2+\tau} + c||e||_{\Delta_x}^{r_2+\tau}, \tag{32}$$

$$\begin{aligned}
& u(\hat{x})(x_2^{\frac{r_1}{r_2}} - (\eta_2 + \eta_1 x_1))\\
& \le c(||\psi||_{\Delta_x}^{r_2+\tau} + ||e||_{\Delta_x}^{r_2+\tau})(c|e_2|^{\frac{r_1}{r_2}} + \eta_1 |e_1|)\\
& \le \frac{1}{8}(\psi_1^{\frac{2r_2}{r_1}} + \psi_2^2) + \tilde{m}_1 e_2^2 + g_2(\eta_1) e_1^{\frac{2r_2}{r_1}}.
\end{aligned} \tag{33}$$

where $\tilde{m}_1$ is a constant.

Now, the third term on the right-hand side of the equation (24) is under discussion. According to inequality (11),

$$\begin{aligned}
& -\eta_1 e_2 (\hat{x}_2 - (\eta_2 + \eta_1 x_1)^{\frac{r_2}{r_1}})\\
& \le -\eta_1 |e_2| \times |(\eta_2 + \eta_1 \hat{x}_1)^{\frac{r_2}{r_1}}\\
& -(\eta_2 + \eta_1 \hat{x}_1 + \eta_1 e_1)^{\frac{r_2}{r_1}}|\\
& \le e_2^2 + \frac{1}{16}\psi_2^2 + \psi_1^{\frac{2r_2}{r_1}} + m_2(\eta_1) e_1^{2r_2/r_1}.
\end{aligned} \tag{34}$$

where $m_2(\eta_1)$ is a continuous function.

Therefore, equation (24) can be rewritten as

$$\dot{U} \le \frac{1}{2}\sum_{i=1}^{2} \psi_i^{\frac{2r_2}{r_i}} - (\eta_1 - 1 - \tilde{m}_1) e_2^2. \tag{35}$$

It is evident that x_2 is unmeasurable, so it will produce a redundant term $\psi_2^{(2r_2-\tau)/(r_2-1)}(u - u^*)$. Next, it need to address this redundant term.

Because u is a C^1 function,

$$u(\hat{x}) - u^*(x) = e_2 \int_0^1 \frac{\partial u(x - \lambda e)}{\partial (x - \lambda e)} d\lambda. \tag{36}$$

The homogeneous degree of $u^*(x)$ is $l_2+\tau$, and the homogeneous degree of $\frac{\partial u(x-\lambda e)}{\partial (x-\lambda e)}$ is τ. Therefore,

$$\frac{\partial u(x - \lambda e)}{\partial (x - \lambda e)} \le c||\psi||_{\Delta_x}^{\tau} + c||e||_{\Delta_x}^{\tau}, \tag{37}$$

$$\psi_2^{\frac{2r_2-\tau}{r_2}-1}(u^*(\hat{x}) - u(x)) \le \frac{1}{4}(\psi_1^{\frac{2r_2}{r_1}} + \psi_2^2) + \tilde{m}_2 e_2^2. \tag{38}$$

where $\tilde{m}_2 \ge 0$.

Constructing a Lyapunov function

$$W = U_2 + V_2. \tag{39}$$

Then

$$\dot{W} \le -\frac{1}{4}(\psi_1^{\frac{2r_2}{r_1}} + \psi_2^2) - (\eta_1 - 1 - \tilde{m}_2 - \tilde{m}_1) e_2^2. \tag{40}$$

Let

$$\eta_1 = \frac{1}{4} + 1 + \tilde{m}_2 + \tilde{m}. \tag{41}$$

then

$$\dot{W} \le -\frac{1}{4}(\psi_1^{\frac{2r_2}{r_1}} + \psi_2^2 + e_2^2). \tag{42}$$

Define the following matrix

$$X = (x_1, x_2, \eta_2)^T. \tag{43}$$

Similarly, from the construction of ψ_i and e_i, it can be inferred that the right-hand side of equation (42) is negatively definite. Therefore, the closed-loop system is globally asymptotically stable.

In addition, the closed-loop system (14) can be rewritten as the following form

$$\dot{X} = F(X) = (x_2, u(\hat{x}), \dot{\eta}_2)^T. \quad (44)$$

One can see that this closed-loop system is homogeneous. Selecting the dilation weight

$$\begin{aligned} \Delta &= (\Delta_x, \Delta_\eta) = (r_1, r_2), \\ \Delta_x &= (1, 1+\tau, 1+2\tau, 1+3\tau), \\ \Delta_\eta &= (1, 1+\tau, 1+2\tau). \end{aligned} \quad (45)$$

One can get that $F(X)$ is the homogeneous of degree τ, W is the homogeneous of degree $2r_2 - \tau$ and the right hand side of (42) is the homogeneous of degree $2r_2$. Then it can be got by Lemma 2 that there is a constant $\tilde{c}$ such that

$$\frac{\partial W(X)}{\partial X} F(X) \leq -\tilde{c}||X||_\Delta^{2r_2}. \quad (46)$$

It has been proven above that a homogeneous output feedback controller can achieve global stability of the system (14). Next, it will be demonstrated that a homogeneous output feedback controller can stabilize the front wheel shimmy system (7).

Firstly, the nonlinear front wheel shimmy system (7) is converted to coordinates, letting $z_1 = x_1$, $z_2 = x_2/L$, $u(\hat{z}) = u(\hat{x})/L^2$. Then the converted nonlinear front wheel shimmy system becomes:

$$\begin{aligned} \dot{z}_1 &= Lz_2 + \varphi_1(t, z, u(\hat{z})), \\ \dot{z}_2 &= Lu(\hat{z}) + \frac{\varphi_2(t, z, u(\hat{z}))}{L}. \end{aligned} \quad (47)$$

The Lyapunov derivative of system (47) is

$$\begin{aligned} \dot{W}_f &\leq -\frac{1}{4}(\xi_1^{2r_2/r_1} + (\xi_j^2 + e_j^2)) \\ &+ \frac{\partial W_f(Z)}{\partial Z}[\varphi_1(z) \quad \frac{\varphi_2(z)}{L}]^T \\ &\leq -LC_1||Z||_\Delta^{2r_2} + \frac{\partial W_f(Z)}{\partial Z}[\varphi_1(z) \quad \frac{\varphi_2(z)}{L}]^T. \end{aligned} \quad (48)$$

Where $Z = [z_1 \quad z_2]^T$.

According to system (7), $\varphi_1(t, x, u) = 0$. Via Hypothesis 1, there exists

$$\begin{aligned} &|\varphi_1(t, z, u(\hat{z}))| = 0, \\ &|\varphi_2(t, z, u(\hat{z}))| \leq c(|z_1|^{\tau+1} + |Lz_2|^{\frac{2\tau+1}{\tau+1}}). \end{aligned} \quad (49)$$

Because of $L \geq 1$, one can further get

$$\begin{aligned} |\varphi_1(t, z, u(\hat{z}))| &= 0, \\ |\frac{\varphi_2(t, z, u(\hat{z}))}{L}| &\leq CL^{1-\frac{1}{\tau+1}}(|z_1|^{\frac{r_2+\tau}{r_1}} + |z_2|^{\frac{r_2+\tau}{r_2}}). \end{aligned} \quad (50)$$

$\frac{\partial W_f(Z)}{\partial Z_i}$ is $2r_2 - \tau - r_i$ degree homogeneous function. According to Lemma 3,

$$\begin{aligned} &|\frac{\partial W_f(Z)}{\partial Z_1}|(|z_1|)^{\frac{r_1+\tau}{r_1}}, \\ &|\frac{\partial W_f(Z)}{\partial Z_2}|(|z_1|^{\frac{r_2+\tau}{r_1}} + |z_2|^{\frac{r_2+\tau}{r_2}}). \end{aligned} \quad (51)$$

is homogeneous of degree $2r_2$.

Via equations (50) and (51), a constant $\lambda_i > 0$ can be found such that

$$\frac{\partial W_f(Z)}{\partial Z_i} \frac{\phi_i(z)}{L^{i-1}} \leq \lambda_i L^{1-\frac{1}{(i-1)\tau+1}}||Z||_\Delta^{2r_2}. \quad (52)$$

Substituting equation (52) into (48), one obtains

$$\dot{W}_f \leq -L(c_1 - \lambda_2 L^{-\frac{1}{\tau+1}})||Z||_\Delta^{2r_2}. \quad (53)$$

From equation (53) , it is obvious that by choosing an appropriate constant L, the Lyapunov function $\dot{W}_f < 0$. So the nonlinear front wheel shimmy system is asymptotically stable under the controller (12) and observer (13).

Sliding mode control (SMC) is used for comparison to verify the effectiveness of the homogeneous domination control method in our simulations.

First, the sliding surface of the SMC is selected as

$$s = \varsigma_1 x_1 + x_2, \quad (54)$$

where ς_1 is a parameter to be specified.

The differentiation of equation (54) is

$$\dot{s} = \varsigma_1 \dot{x}_1 + \dot{x}_2. \quad (55)$$

The control rate is

$$\dot{s} = -\varsigma_2 \operatorname{sgn}(s), \quad (56)$$

where $\varsigma_2 > 0$, $sgn(s) = \begin{cases} 1, s > 0 \\ 0, s = 0 \\ -1, s < 0 \end{cases}$.

By combining equation (55) and (56), $\varsigma_1 \dot{x}_1 + \dot{x}_2 = -\varsigma_2 \operatorname{sgn}(s)$. Then, substituting $\dot{x}_1$ and $\dot{x}_2$ (see equation (7)) into the equation, one obtains the sliding mode controller (57) as

$$\begin{aligned} u_{smc} = &-[d^2 k_s + d^2 k_z \sin\alpha(\sin\alpha + f\cos\alpha) \\ &+ k\chi(t_m + R\sin\alpha)]x_1 - [c_l + d^2 c_s \\ &- bk\chi(t_m + R\sin\alpha)]x_2 + [a_1\chi(x_1 - bx_2) \\ &+ a_2\chi^2(x_1 - bx_2)^2 + a_3\chi^3(x_1 - bx_2)^3] \\ &(t_m + R\sin\alpha) + \Delta + J\varsigma_1 x_2 + J\varsigma_2 \operatorname{sgn}(s). \end{aligned} \quad (57)$$

5. SIMULATION ANALYSIS

In this section, MATLAB/Simulink is utilized to develop a one-degree-of-freedom front wheel shimmy model for simulation purposes. This simulation aims to verify the effectiveness of the designed homogeneous domination controller and to assess the observer's performance. The simulations were carried out under various operating conditions, with vehicle speeds of 60 km/h and 100 km/h. Additionally, the simulation took into account unknown sensor measurement errors, modeled as f(t)=1+0.5sin(10t), which suggests that sensor errors oscillate within the range [0.5, 1.5]. Table 1 lists the primary parameters of the vehicle. Table 2 and Table 3 respectively list the parameters for homogeneous domination control and sliding mode control.

5.1 Step signal disturbance

A step signal of θ=0.2 rad is applied to the front wheel at the 5th second as a disturbance. Figs. 3 to 7 respectively illustrate the actual, observed values, and controller outputs for the shimmy angle and its derivative under various vehicle speeds.

From Figs. 3 and 5, it can be observed that after the step signal disturbance is applied, the shimmy angle rapidly decreases from 0.2 rad. However, there is a difference in the magnitude of the second peak of the shimmy angle; in Fig. 3, it is 0.1 rad, whereas in Fig. 5, it is 0.05 rad. It is also observable that the shimmy angle can be swiftly suppressed under different vehicle speeds, and it ultimately approaches 0 rad without a subsequent increase. At a speed of 60 km/h, it takes 1.3 seconds for suppression, while at 100 km/h, it requires only 1.1 seconds. Consequently, it is evident that at higher vehicle speeds, the shimmy angle is suppressed more rapidly, and the shimmy phenomenon is more readily mitigated. Additionally, the designed observer is capable of accurately estimating the actual values, with the error between the actual value (θ) and observed value ($\hat{\theta}$) relatively small.

Figs. 4 and 6 depict the derivative of shimmy angle and its observed value. They reflect the rate of change of the shimmy angle. It can be observed from the figures that at a vehicle speed of 60 km/h, the maximum peak value of the derivative of shimmy angle is -7 rad/s, and at a speed of 100 km/h, it is -5.5 rad/s. When it approaches zero, it also corresponds to the time when the shimmy angle approaches zero, which is also indicated by the results in the figures.

The controller output, shown in Fig. 7. At a vehicle speed of 60 km/h, the maximum output of the controller is approximately 32 Nm, and at a speed of 100 km/h, it is 29 Nm. It indicates the robustness of the designed homogeneous domination controller.

Therefore, it can be concluded that under a step signal of θ=0.2 rad and varying vehicle speeds, the homogeneous domination control method effectively mitigates issues related to unknown sensor sensitivities and nonlinear model terms, successfully suppressing the shimmy phenomenon.

Table 1. The main parameters of the model

Name	Symbol	Unit	Value
Vehicle mass	m	kg	1400
Effective length of steering knuckle	L	m	0.15
Equivalent torsional stiffness of the wheel around kingpin	k_s	N m/rad	40000
Vertical stiffness of tires	k_z	N/m	120000
Tire cornering stiffness	C_r	N/rad	15700
The moment of inertia of the wheel around kingpin	J	kg·m^2	10

Table 2. Homogeneous domination control parameters

Parameters	Value	Parameters	Value
r_1	1.1	k_1	24
r_2	1.05	l_1	5
β_1	1	β_2	5
τ	0.02		

Table 3. Sliding mode control parameters

Parameters	Value
ς_1	5
ς_2	0.14

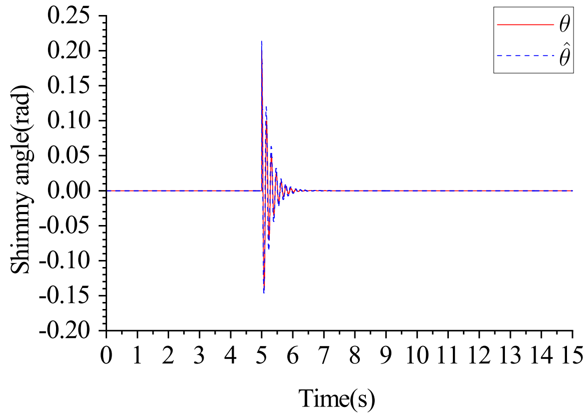

Fig. 3. Trajectories of the θ and $\hat{\theta}$ under v=60km/h suffering θ=0.2 rad

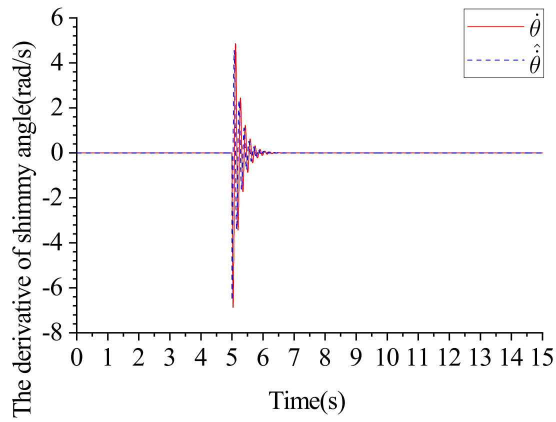

Fig. 4. Trajectories of the $\dot{\theta}$ and $\dot{\hat{\theta}}$ under v=60km/h suffering θ=0.2 rad

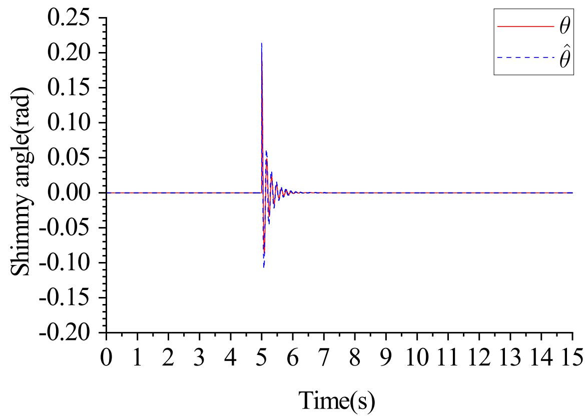

Fig. 5. Trajectories of the θ and $\hat{\theta}$ under v=100km/h suffering θ=0.2 rad

5.2 L2 disturbance

A time-varying signal, given by L_2=20sin(15t)/(1+t^2), is applied to the front wheel commencing from the 5th second. Similarly, Figs. 8 to 12 respectively illustrate the

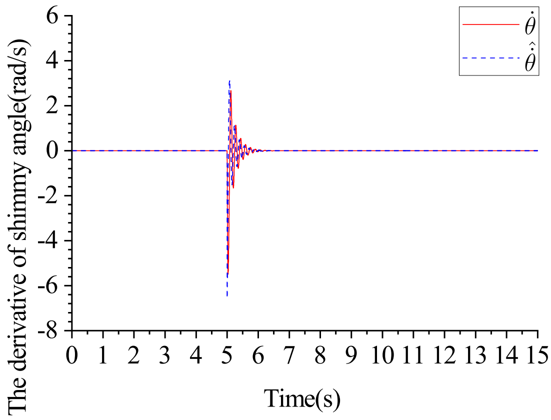

Fig. 6. Trajectories of the $\dot{\theta}$ and $\hat{\dot{\theta}}$ under v=100km/h suffering θ=0.2 rad

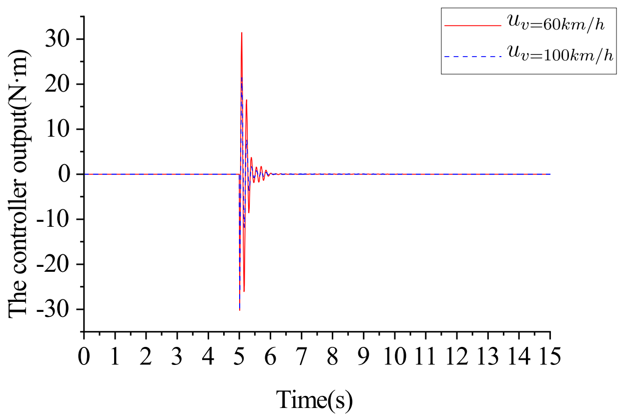

Fig. 7. The controller output under v=60km/h and 100km/h suffering θ=0.2 rad

actual, observed values, and controller outputs for the shimmy angle and its derivative under various vehicle speeds.

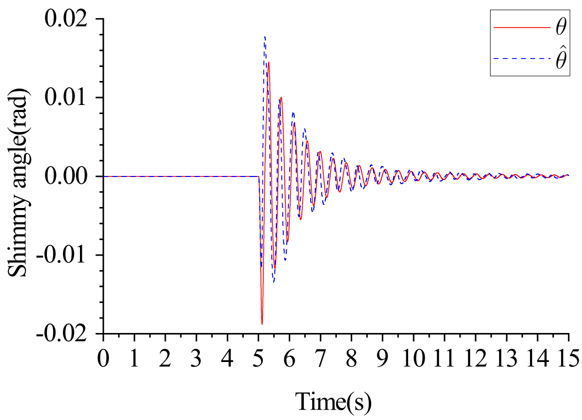

Fig. 8. Trajectories of the θ and $\hat{\theta}$ under v=60km/h suffering L_2=20sin(15t)/(1+t^2) disturbance

In Figs. 8 and 10, it can be observed that when the vehicle speed is 60 km/h, the maximum amplitude of the shimmy angle is 0.018 rad, and when the vehicle speed is 100 km/h, it is 0.014 rad. The amplitude of the shimmy angle is

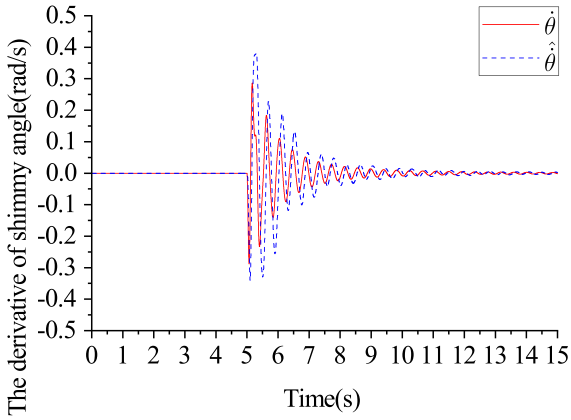

Fig. 9. Trajectories of the $\dot{\theta}$ and $\hat{\dot{\theta}}$ under v=60km/h suffering L_2=20sin(15t)/(1+t^2) disturbance

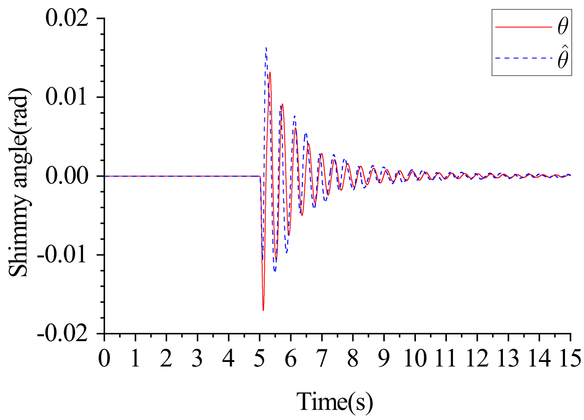

Fig. 10. Trajectories of the θ and $\hat{\theta}$ under v=100km/h suffering L_2=20sin(15t)/(1+t^2) disturbance

slightly larger at lower vehicle speeds. Additionally, the time taken for the shimmy angle to approach and stabilize near 0 is comparable for both speeds, being approximately 7 seconds. Similarly, Figs. 9 and 11 depict the derivative values of the shimmy angle. At a vehicle speed of 60 km/h, the maximum amplitude is 0.3 rad/s, and at 100 km/h, it is 0.26 rad/s. It is evident from Figs. 8 to 11 that the observer is capable of effectively tracking the actual values, yielding satisfactory results. From Fig. 12, it can be observed that the controller outputs are quite similar; however, the maximum torques produced are different. At a vehicle speed of 60 km/h, the maximum output is 3 Nm, whereas at 100 km/h, it is 2.7 Nm.

Therefore, it can be concluded that under the disturbance of L_2=20sin(15t)/(1+t^2) at varying vehicle speeds, the homogeneous domination control method effectively addresses the challenges posed by unknown sensor sensitivities and nonlinearities within the model, effectively eliminating shimmy phenomenon.

5.3 Comparison with SMC

To better demonstrate the advantages of the Homogeneous Domination Control (HDC) method, this study conducted a comparative analysis with the Sliding Mode Control (SMC) method.

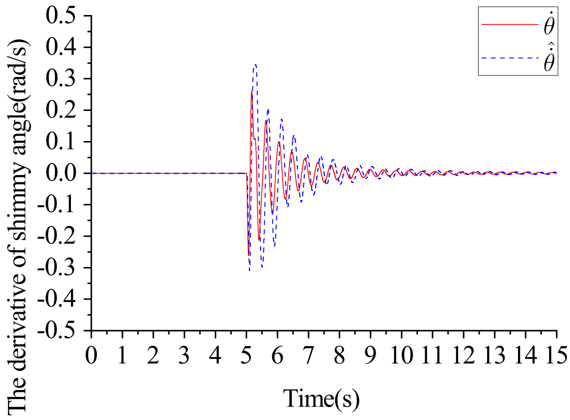

Fig. 11. Trajectories of the $\dot{\theta}$ and $\dot{\hat{\theta}}$ under v=100km/h suffering L_2=20sin(15t)/(1+t^2) disturbance

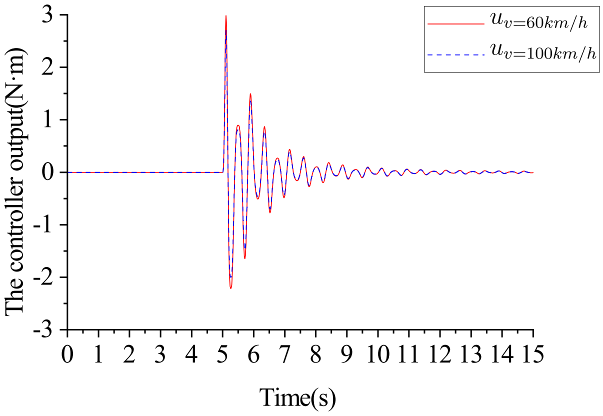

Fig. 12. The controller output under v=60km/h and 100km/h suffering L_2=20sin(15t)/(1+t^2) disturbance

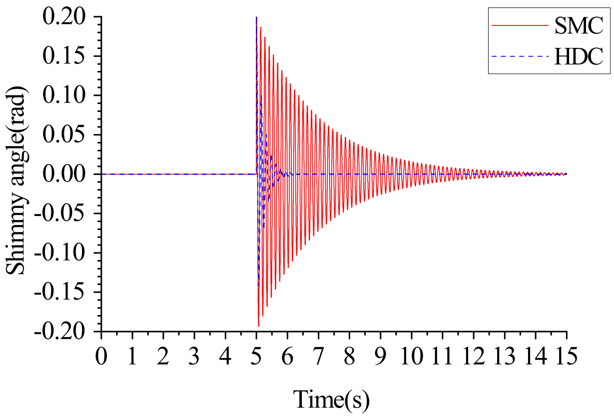

Fig. 13. The comparison of θ with different controller under v=60km/h suffering θ=0.2 rad

Figs. 13 and 14 illustrate the comparison of the shimmy angle under various vehicle speeds and control strategies when subjected to a disturbance with an angular displacement of θ=0.2 rad. Figs. 13 and 14 illustrate that at a vehicle speed of 60 km/h, the homogeneous domination control eliminates the shimmy angle in 1.3 seconds, whereas the sliding mode control requires 9 seconds. Moreover, under SMC, the decay rate of the shimmy angle is significantly slower compared to that under HDC. At a vehicle speed of 100 km/h, the situation is similar; HDC requires 1.1 seconds to eliminate the shimmy angle, while SMC demands 4.5 seconds. Figs. 15 and 16 show the comparison of the shimmy angle under different vehicle speeds and control methods when a L_2=20sin(15t)/(1+t^2) disturbance is applied. Overall, the decay trend of the shimmy angle is similar; however, the amplitude of the peaks is noticeably larger under sliding mode control. At a vehicle speed of 60 km/h, the shimmy angle stabilizes by the tenth second with homogeneous domination control, but only by the twelfth second with SMC. Additionally, it can be observed that the rate of change of the shimmy angle is smoother under HDC, which implies better vehicle stability.

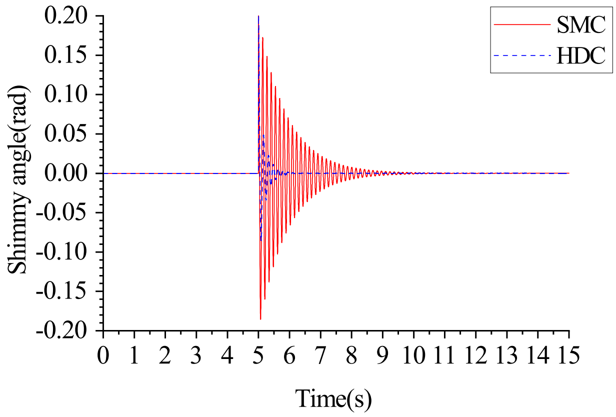

Fig. 14. The comparison of θ with different controller under v=100km/h suffering θ=0.2 rad

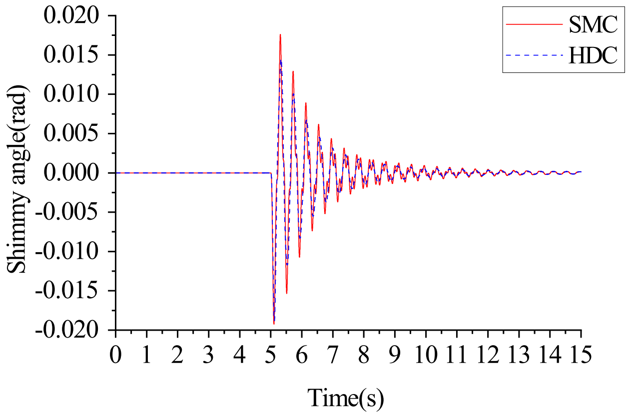

Fig. 15. The comparison of θ with different controller under v=60km/h suffering L_2=20sin(15t)/(1+t^2) disturbance

In summary, both homogeneous domination control and sliding mode control are capable of suppressing the shimmy angle, demonstrating the effectiveness of both control methods. However, upon comparison, it is evident that the superiority of HDC significantly surpasses that of SMC. This reaffirms the rationality of the selection of HDC to address the shimmy phenomenon in this study.

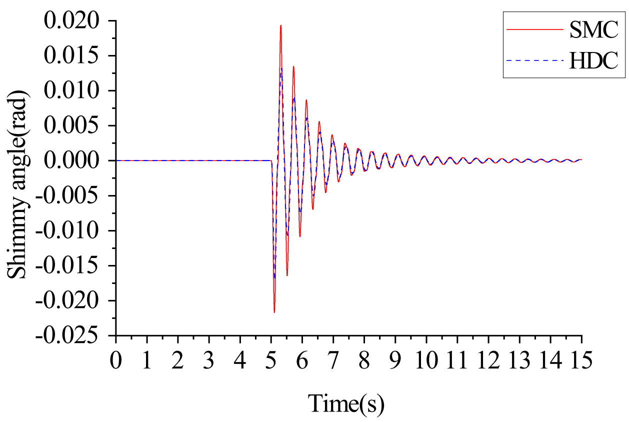

Fig. 16. The comparison of θ with different controller under v=100km/h suffering L_2=20sin(15t)/(1+t^2) disturbance

6. CONCLUSION

To address the front wheel shimmy issue in electric wheeled vehicles, considering unknown sensor measurement errors and nonlinearity, this paper introduces an active shimmy control method. A one-degree-of-freedom front wheel shimmy model is developed for the control system. Homogeneous theory is utilized in the control strategy, leading to the design of a homogeneous domination-based observer and controller. The Lyapunov method is employed to demonstrate that the designed controller can globally asymptotically stabilize the system. Numerical simulations indicate that the observer can accurately estimate the system states, and the controller effectively suppresses the shimmy angle. A sliding mode control (SMC) method is also simulated for comparison with the homogeneous domination control (HDC) method. The comparison reveals that the HDC provides superior performance in terms of suppression effectiveness and stability compared to SMC.

ACKNOWLEDGMENTS

The work is partially supported by Zhejiang Provincial Natural Science Foundation of China under Grant No.LZ21E050002.

REFERENCES

Ata, B., and Coban, R. (2022). Decoupled adaptive backstepping sliding mode control of underactuated mechanical systems. Journal of Control Engineering and Applied Informatics, 24(1), 45-56.

Becker, Fromm, and Maruhn. (1931). Vibrations of the Steering Systems of Automobiles. Kr-ayn. Berlin. M.R.

Bakker, E., Nyborg, L., and Pacejka, H.B. (1987). Tyre modelling for use in vehicle dynamics studies. SAE[C], 870421.

Chen, C.C., and Xu, S.S.D. (2018). Global stabilization for a class of genuinely nonlinear systems with a time-varying power: An interval homogeneous domination approach. IEEE Access, 6, 11255-11264.

Demic, M. (1996). Analysis of influence of design parameters on steered wheels shimmy of heavy vehicle. Vehicle System Dynamic, 26(5), 343-362.

Dong, L., Chen, Z., and Sun, M. (2023). Phase compensation active disturbance rejection control for shimmy vibration with magnetorheological damper of aircraft. Expert Systems with Applications, 213, 119126.

Guo, K.H., Wang, Y., Liu, Y., and Wang, X. (1986). Semi-Empirical Model of Tire Lateral Characteristics. Automotive Engineering, 10(2), 44-54.

Guo, K.H. (1995). Influence of Tire Dynamic Lateral Characteristics on Vehicle Shimmy. Automotive Technology, 4, 1-6.

He, L. (2004). A simulation calculation research on front wheel shimmy for automobile. Hebei University of Technology.

Kawski, M. (1990). Homogeneous stabilizing feedback laws. Control theory and advanced technology, 6(4), 497-516.

Kchaou, M., Jerbi, H., Abbassi, R., Aoun, S. B., and VijiPriya, J. (2022). Reliable sampled-data fuzzy control for non-linear systems. Journal of Control Engineering and Applied Informatics, 24(4), 3-12.

Lu, H., Lu, J., and Wei, H. (2023). On the non-linear dynamics of vehicle shimmy coupled with handling motions: modelling, bifurcation analysis, and validations. Journal of Vibration and Control, 29(15-16), 3435-3450.

Meng, Q., Qian, C., and Shu, Y. (2019). Active steering wheel shimmy control for electric vehicle by sampled-data output feedback. ISA transactions, 84, 262-270.

Meng, Q., Qian, C., and Hu, C. (2020). Finite-time active shimmy control based on uncertain disturbance observer for electric vehicle with independent suspension. IET Intelligent Transport Systems, 14(13), 1835-1844.

Meng, Q., Chen, C.C., and Wang, P. (2021). Study on vehicle active suspension system control method based on homogeneous domination approach. Asian Journal of Control, 23(1), 561-571.

Meng, Q., Sun, Z., and Shen, Z. (2023). Homogeneous domination-based lane-keeping control method for intelligent vehicle. Nonlinear Dynamics, 111(7), 6349-6362.

Meng, Q., Zhao, S., Liu, R., Sun, Z. Y., and He, H. (2024). Active Shimmy Control Method for Driverless Electric Vehicle Considering Unknown Sensor Measurement Error via Sampled-data Output Feedback. IEEE Access.

Pacjka, H.B. (1966). The wheel shimmy phenomenon. Netherland: Delft University of Technology.

Pacjka, H.B. (1973). Approximate Dynamic Shimmy Response of Pneumatic Tires. Vehicle System Dynamics.

Qian, C. (2005). A homogeneous domination approach for global output feedback stabilization of a class of nonlinear systems. In Proceedings of the 2005, American Control Conference, 4708-4715. IEEE.

Qian, C.J. and Li, J. (2006). Global output feedback stabilization of upper-triangular nonlinear systems using a homogeneous domination approach. International Journal of Robust and Nonlinear Control: IFAC-Affiliated Journal, 16(9), 441-463.

Wang, X.X., Wang, Y., and Xin, J.X. (2012). Influence of Tire Parameters on Front Wheel Shimmy. Journal of Hubei Automotive Industry Institute, 26(02), 1-4+8.

Wang, Y., Jin, X., and Yin, Y. (2022). Using nonlinear feedback control to improve aircraft nose landing gear shimmy performance. Meccanica, 57(9), 2395-2411.

Wei, H., Lu, J.W., and Jiang, J.Z. (2022). Analysis of Dynamic Behavior of Vehicle Shimmy System with

Stochastic Clearance. Mech Sol, 57(1), 139-48.

Wu, J., Wang, Z., Zhang, L., and Ding, X. (2023). Research on Coordinated Control Strategy for the Longitudinal and Lateral Stability of Four-Wheel Hub Motor-Driven Electric Vehicles. Journal of Mechanical Engineering, 59(04), 163-172.

Wang, Y., Zhang, T., and Jin, X. (2023). Shimmy suppression of an aircraft nose landing gear using torsional nonlinear energy sink. Journal of Computational and Nonlinear Dynamics, 18(10).

Wang, Y., Xu, B., and Meng, H. (2024). Enhanced vehicle shimmy performance using inerter-based suppression mechanism. Communications in Nonlinear Science and Numerical Simulation, 130, 107800.

Xie, X.J. and Liu, L. (2012). A homogeneous domination approach to state feedback of stochastic high-order nonlinear systems with time-varying delay. IEEE Transactions on Automatic Control, 58(2), 494-499.

Xiao, C. (2022). A Method for Suppressing Vehicle Steering Wheel Shimmy Based on Rack Force Estimation. Auto Parts, 10, 51-54.

Zhao, G., Su, Z.G., and Sun, Z.Y. (2020). Homogeneous domination control for uncertain nonlinear systems via interval homogeneity with monotone degrees. IEEE Access, 8, 48632-48641.

Zhuang, X. (2020). Research on the Development Status and Trends of Drive Motors for New Energy Vehicles. Era Automobile, 01, 47-48.

Zhou, J.C. (2022). Control of Single-Axis Steering Mechanism for Overhead Single-Track Vehicle Shimmy. Chongqing Jiaotong University.

Zhang, X., Zhang, Y., Hu, Q., Yang, A., and Li, X. (2023). Fixed-Time Command-Filtered Adaptive Backstepping Control for a Class of Uncertain MIMO Systems.. Journal of Control Engineering and Applied Informatics, 25(4), 3-13.